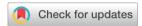
ChemComm



COMMUNICATION



Cite this: Chem. Commun., 2022, **58**. 11855

Received 17th June 2022, Accepted 28th September 2022

DOI: 10.1039/d2cc03399b

rsc.li/chemcomm

Highly diastereo- and branched-selective rearrangement of substituted N-alloc-N-allyl ynamides†

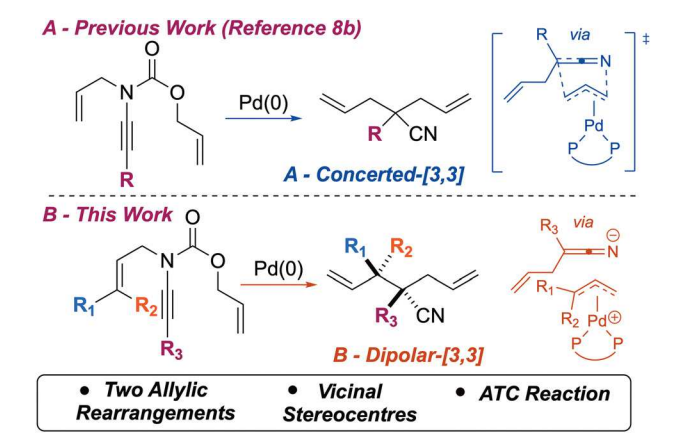
Oliver D. Jackson, Ksenia S. Stankevich and Matthew J. Cook *

An auto-tandem catalytic, branched-selective rearrangement of substituted N-alloc-N-allyl ynamides was developed. This reaction provides ready access to complex quaternary nitrile products with vinylogous stereocentres in excellent diastereoselectivity, including contiguous all-carbon quaternary centres. The stereochemical outcome is determined via a Pd(0) catalysed dipolar ketenimine aza-Claisen rearrangement and computational studies exemplify the key role ligand geometry plays.

Using a single catalyst to perform multiple, mechanistically distinct reactions (auto-tandem catalysis [ATC])¹ can be a very powerful approach in synthesis.² ATC reactions are particularly impactful when multiple C-C bonds are formed,³ especially if stereogenic elements are generated during these processes. Of particular interest is the formation of all-carbon quaternary centres using ATC approaches.4

The high reactivity and linear geometry of unstabilized nitrile anions have made them problematic in many catalytic reactions. Lewis basic additives (to form aggregated complexes),⁵ decarboxylative/deacylative approaches, and silyl ketenimines have all been utilized, however many challenges remain. Our contribution to the field was developing a Pd-catalysed rearrangement of N-alloc-N-allyl ynamides which formed quaternary diallyl nitriles (Scheme 1A). 8,9 This ATC process performs two mechanistically distinct allylic rearrangements and avoids requirement for nitrile anion intermediates. During this study we discovered that Pd(0) was acting as a nucleophilic catalyst, donating electron density into the σ_{C-N}^* orbital triggering a concerted [3,3]-rearrangement (Scheme 1A). In contrast, other Pd-catalysed aza-Claisen rearrangements proceed through a π -Lewis acidic Pd(II) pathway. We reasoned that substrates encompassing γ -substituted N-allyl groups would provide branched products containing two contiguous stereogenic centres in this reaction.

Department of Chemistry and Biochemistry, Montana State University, Bozeman, MT 59717, USA. E-mail: matthewcook@montana.edu



Scheme 1 ATC rearrangement of N-alloc-N-allyl ynamides with unsubstituted (A) and substituted (B) allyl groups.

Moreover, if substrates include γ , γ -disubstitution, contiguous all-carbon quaternary stereocentres could be formed. Importantly, these are mechanistically distinct from previously disclosed branched-selective allylations.¹¹ Herein, we report the development of a highly diastereoselective ATC reaction with complete branched selectivity under very mild conditions (Scheme 1). Of particular note is the dipolar allyl ketenimine-[3,3]-rearrangement which achieves high levels of diastereoselectivity, including the formation of vicinal all-carbon quaternary stereocentres (Scheme 1B).

Optimization studies revealed that a variety of bidentate phosphine ligands provided complete branched selectivity (2a). Of note, were catalytic systems derived from Pd2dba3 and phosphine ligands (L1-3) due to the abundance of commercially available variants (Table 1). Unsubstituted phenyl, alkyl and furyl substituted ligands (L1a-c) gave poor reactivity and selectivity (entries 1-3). Ligands containing 3,5-disubstituted phenyl groups (L1d-e) led to improved selectivity (entries 4 and 5). The addition of electron donating groups at the 4-position (L1f-h), improved both yield and selectivity (entries 6-8), with DTBM-MeOBiphep (L1g) proving optimal. Other DTBM substituted

[†] Electronic supplementary information (ESI) available. See DOI: https://doi.org/ 10.1039/d2cc03399b

¹H NMR of crude.

Communication ChemComm

Table 1 Selected optimization studies^a

Entry	Ligand	$Yield^{b}$ (%)	$d.r.^d$
1	(R)-MeOBiphep (L1a)	11	1.8:1
2	(R)-i-Pr-MeOBiphep (L1b)	5	1:1.2
3	(R)-Fur-MeOBiphep (L1c)	35	1:1.1
4	(R)-DM-MeOBiphep (L1d)	8	3.6:1
5	(R)-DTB-MeOBiphep (L1e)	20	5.4:1
6	(R)-DMM- MeOBiphep (L1f)	40	9:1
7	(R)-DTBM-MeOBiphep (L1g)	$70 (63)^c$	13:1
8	(R)-iPr-Me ₂ N-MeOBiphep (L1h)	57	13:1
9	(R)-DTBM-Segphos (L2g)	15	13:1
10	(R)-DTBM-Garphos $(L3g)$	25	5:1
		OMe	

3,5-Me-4-MeO-Ph (f); 3,5-t-Bu-4-MeO-Ph (g); 3,5-i-Pr-4-Me₂N-Ph (h) ^a For detailed optimization studies, see ESI. ^b Determined by ¹H NMR using mesitylene as internal standard. ^c Isolated yield. ^d Determined by

ligands (L2g/3Lg, entries 9 and 10) also provided selectivity, but with poor reactivity.

With the optimized conditions in hand (Table 1, entry 8), we began examining the substrate scope (Scheme 2). Substitution on the ynamide phenyl group was investigated and the stereochemical outcome appears to be influenced by the mesomeric stabilization of an anion, 12 suggesting a dipolar mechanism (Scheme 1B). Weakly π -donating groups, such as fluorine (1b, σ = -0.03), gave lower selectivity than **1a**, whereas strongly anion stabilizing groups including CF₃ (1c, σ = 0.65), NO₂ (1d σ = 1.27), and CN (1e, σ = 1.00) provided very high levels of stereoselectivity ($\geq 26:1$ d.r.). Next our attention turned to modulation of the γ -substituted N-allyl group. Basic heterocycles could be tolerated in this reaction with pyridine (1f) and quinoline (1g) variants providing high yields and diastereocontrol. Other substitution could be tolerated on the migrating allylic group, with electron deficient groups providing excellent outcomes. 4-Nitro (1h), 3,4,5-trifluoro (1i), and 3,5-bis-(trifluoromethyl) (1j) substrates all gave high chemical yields with exquisite diastereoselectivity.

 γ, γ -Disubstituted *N*-allyl groups were also examined, which upon rearrangement, produced highly congested vicinal all-carbon quaternary centres. Cycloalkyl and thiopyranyl substituted ynamides (1k-m) variants gave highly efficient routes to cyclic branched nitriles 2k-m. We also investigated diastereoselectivity in the formation of contiguous all-carbon quaternary centres. Facial selectivity on the N-allyl group was probed by

Scheme 2 Substrate scope. a Isolated yield. Determined by ¹H NMR. c 2l produced in 16% ee

installing a 4-tert-butyl cyclohexyl group (1n), which provided the 2n in 15:1 d.r. The formation of two contiguous all-carbon stereogenic centres could also be achieved, with tetralone derived ynamide 10 providing nitrile 20 in good yield and an impressive 13:1 d.r. This example (10 to 20) demonstrates the power of this approach in forming very congested C-C bonds as part of an auto-tandem catalytic sequence with high-levels of diastereoselectivity.

The stereospecificity of this reaction was further investigated by comparing the relative outcomes using E and Z-carbamates E-1p and Z-1p (Scheme 3A). Both reactions proceeded with similar chemical efficiency, however E-1p provided a 3:1 mixture of diastereomers (2p:2p'), whereas the **Z-1p** resulted in a 1.2:1 ratio. These outcomes demonstrate stereospecificity, albeit with a competing isomerization pathway. This π – σ – π pathway is a common source of low stereoselectivity with acyclic Z- π -allyl donors.¹³ Interestingly, γ,γ-diphenyl substituted allyl ynamide

ChemComm

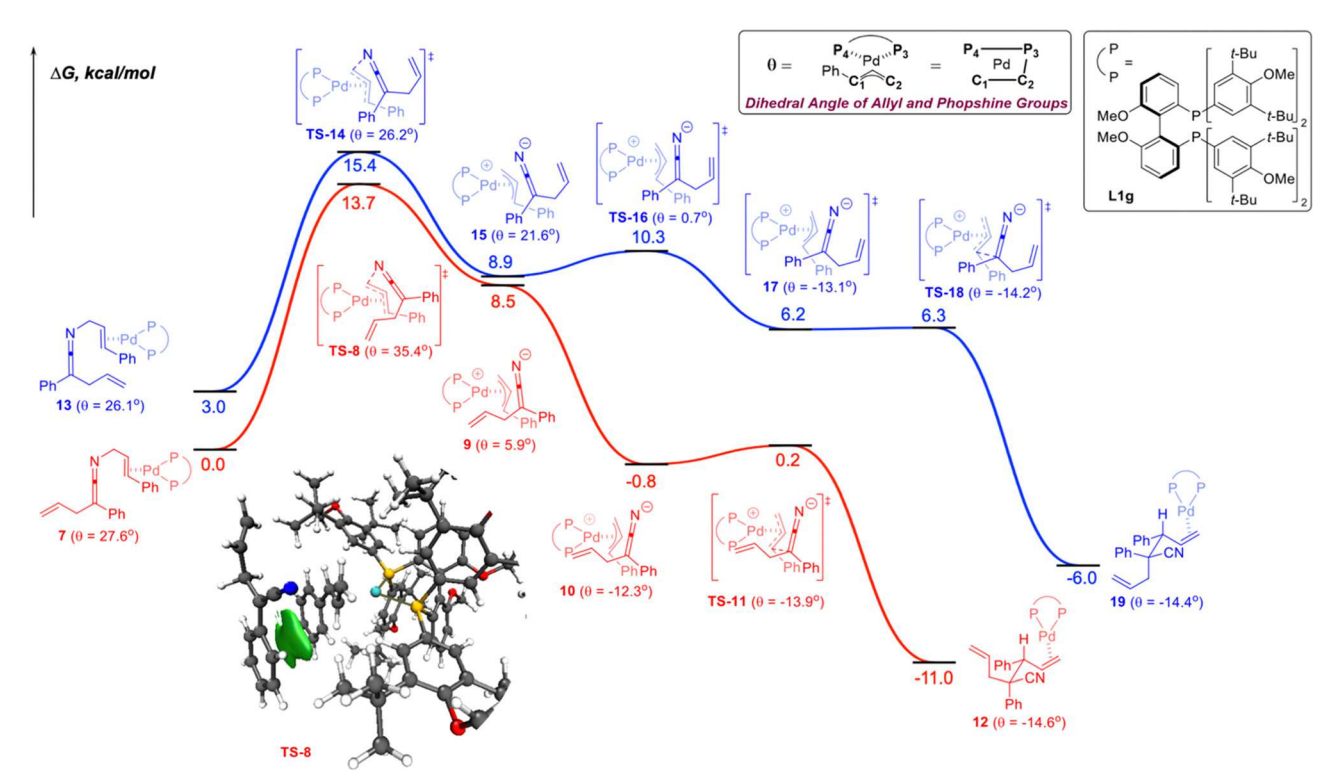
1q

A - Alkene Stereospecificity Me 2.5 mol% Pd₂dba₃ 2.5 mol% Pd₂dba₃ 6 mol% L1g 6 mol% L1q 0.25 equiv. Et₃B 0.25 equiv. Et₃B 1 equiv. N, O-BSA 1 equiv. N, O-BSA ĆN CN. PhCF₃, 60 °C, 16 h PhCF₃, 60 °C, 16 h 2p 2p' E-1p Z-1q 59%, 3:1 d.r. 64%, 1.2:1 d.r. B - Diaryl Allyl Substitution C - Spirocyclic Nitrile Formation 2.5 mol% Pd₂dba₃ Ph 6 mol% L1g 5 mol% Grubbs II 0.25 equiv. Et₃B CH2Cl2, 40 °C, 6 h ´CN ´CN 1 equiv. N, O-BSA 2k 4, 76% PhCF₃, 60 °C, 16 h 3, 42% (I-only)

Scheme 3 Additional allylic substitution and synthetic utility studies: (A) alkene stereospecificity, (B) diaryl allyl substitution and (C) spirocyclic nitrile formation.

1q provided the only example where linear selectivity was achieved, affording nitrile 3 as a single isomer (Scheme 3B). This alternative regiochemistry can be rationalized due to the increased conjugation of the linear isomer and the additional steric encumbrance in the branched product. Indeed, only one example of branched selectivity from a 1,1-diphenyl π -allyl metal species has been reported. ¹⁴ The cyclic products could be converted in to spirocycles using Grubb's 2nd generation catalyst to form [5,5]-spirocycle 4 in excellent yield (Scheme 3C).15

To elucidate the origin of diastereoselectivity, we conducted a DFT study of the formation of 2a at CPCM(Trifluorotoluene) M06L/BSII//ONIOM(M06L/BSI:PM6) level of theory (for BSI and BSII see Scheme 4 footnote). We found that the palladium bound ligand (L1g) forms a deep cleft in which reactivity occurs. This conformational restriction results in a dissociative formal process rather than a concerted [3,3]-rearrangement.8b Although ketenimines are stereogenic, they are highly epimerizable and exist as a dynamic mixture of isomers. 16 Allyl ketenimine coordinates deep within the binding pocket, forming



Scheme 4 Summary of DFT analysis examining the diastereoselectivity in the formation of 2a. a DFT calculations done at CPCM(trifluorotoluene) M06L/ BSII//ONIOM(M06L/BSI:PM6), where BSI = 6-31+G(d) (C, H, P, O)/LANL2DZ (ECP Pd) and BSII = 6-311++G(2d,2p) (C, H, P, O)/LANL2DZ (ECP Pd); ^b Quasi-harmonic solvent and temperature (333.15 K) corrected Gibbs free energies at 1 mol L^{-1} standard state are reported; ^c For optimised structures, see ESI.†

Communication ChemComm

diastereomeric complexes 7/13. These interconvertible complexes (7/13) ionise though transition states TS-8/TS-14, determining the stereochemistry and forming ion pairs 9/15. A possible explanation for this selectivity is the coplanarity of the phenyl groups leading to an offset π -stacking interaction (3.5 Å) in **TS-8** that is not present in TS-14.¹⁷ Indeed, an IGM 3D plot showed an isosurface consistent with a non-covalent stabilizing interaction between the two aromatic rings in TS-8 (see ESI† for full details). 18 The possibility of competing concerted [3,3]-process was considered;8b however, 7/13 do not have the necessary orbital overlap and no [3,3]-transition state could be located. The dihedral angle between the allylic termini and the phosphines can be used to highlight the conformational changes required between C-N bond breaking and C-C bond formation. Following ionisation, the two reaction pathways diverge for C-C bond formation. In the major pathway, ionpair 9 (5.9°) undergoes a reorganisation of the ligand, rotating the π -allyl group within the cleft. Initially, intermediate **10** (-12.3°) is formed, which is in reactive conformation for C-C formation via **TS-11** $(-13.9^{\circ}; +1.0 \text{ kcal mol}^{-1} \text{ from } 10)$, to afford 12. In contrast, ion pair 15 (21.6°) is much further from the reactive conformation for C-C bond formation, requiring rotation through TS-16 (0.7°; +1.4 kcals mol⁻¹ from 15). This produces shallow intermediate 17 (-13.1°) before proceeding directly into a C-C bond formation via **TS-18** $(-14.2^{\circ}, 0.1 \text{ kcal mol}^{-1} \text{ from } 17)$, to form nitrile 19. Despite the dipolar pathway, the ion pair does not fully dissociate or solvent separate, with the energetics suggesting a very rapid C-C bond formation following ionisation.

In conclusion, a highly diastereoselective ATC method for the construction of stereochemically complex nitriles has been developed. This provides a highly attractive route to nitriles containing an all-carbon quaternary stereocentre and further vicinal substitution, including contiguous all-carbon quaternary stereocentres. In addition, we have developed a highly accurate computational model to deconvolution of the ketenimine rearrangement mechanism, including the discovery of a dipolar [3,3]-process which occurs in a deep cleft within the catalyst.

Research supported by NSF (CHE-1800487). Calculations performed on Expanse through XSEDE (CHE-200093/CHE-200121). NSF (DBI-1532078/CHE-2018388) and Murdock Charitable Trust Foundation (2015066:MNL) provided funds for 400 and 500 MHz NMR spectrometers used in this research.

Conflicts of interest

There are no conflicts to declare.

Notes and references

- 1 D. E. Fogg and E. N. dos Santos, Coord. Chem. Rev., 2004, 248, 2365.
- 2 (a) J. E. Camp, Eur. J. Org. Chem., 2017, 425; (b) N. T. Patil, V. S. Shinde and B. A. Gajula, Org. Biomol. Chem., 2012, 10, 211; (c) A. R. O. Venning, M. R. Kwiatkowski, J. E. Roque Peña, B. C. Lainhart, A. A. Guruparan and E. J. Alexanian, J. Am. Chem. Soc., 2017, 139, 11595; (d) C. Zhou, J. Jiang and J. Wang, Org. Lett., 2019, 21, 4971.
- 3 (a) P. Chen, Z.-C. Chen, Y. Li, Q. Ouyang, W. Du and Y.-C. Chen, Angew. Chem., Int. Ed., 2019, 58, 4036; (b) J. Long, R. Yu, J. Gao and X. Fang, Angew. Chem., Int. Ed., 2020, 59, 6785-6789; (c) M.-Z. Wang, C.-Y. Zhou and C.-M. Che, Chem. Commun., 2011, 47, 1312.
- 4 (a) C. J. Douglas and L. E. Overman, Proc. Natl. Acad. Sci. U. S. A., 2004, 101, 5363; (b) K. W. Quasdorf and L. E. Overman, Nature, 2014, **516**, 181; (c) J. P. Das and I. Marek, Chem. Commun., 2011, 47, 4593; (d) J. Feng, M. Holmes and M. J. Krische, Chem. Rev., 2017, 117, 12564-12580; (e) E. A. Peterson and L. E. Overman, Proc. Natl. Acad. Sci. U. S. A., 2004, 101, 11943.
- 5 (a) Z. Jiao, K. W. Chee and J. S. Zhou, J. Am. Chem. Soc., 2016, 138, 16240; (b) B. W. H. Turnbull and P. A. Evans, J. Am. Chem. Soc., 2015, 137, 6156.
- 6 (a) A. Recio and J. A. Tunge, Org. Lett., 2009, 11, 5630; (b) A. J. Grenning and J. A. Tunge, J. Am. Chem. Soc., 2011, 133, 14785.
- 7 S. E. Denmark and T. W. Wilson, Angew. Chem., Int. Ed., 2012, 51, 9980.
- 8 (a) J. R. Alexander and M. J. Cook, Org. Lett., 2017, 19, 5822; (b) J. R. Alexander, V. I. Shchepetkina, K. S. Stankevich, R. J. Benedict, S. P. Bernhard, R. J. Dreiling and M. J. Cook, Org. Lett., 2021, 23, 559.
- 9 (a) K. A. DeKorver, H. Li, A. G. Lohse, R. Hayashi, Z. Lu, Y. Zhang and R. P. Hsung, Chem. Rev., 2010, 110, 5064; (b) G. Evano, A. Coste and K. Jouvin, Angew. Chem., Int. Ed., 2010, 49, 2840; (c) C. C. Lynch, A. Sripada and C. Wolf, Chem. Soc. Rev., 2020, 49, 8543.
- 10 (a) H. Bao and U. K. Tambar, J. Am. Chem. Soc., 2012, 134, 18495; (b) J. S. Cannon and L. E. Overman, Acc. Chem. Res., 2016, 49, 2220; (c) A. M. Danowitz, C. E. Taylor, T. M. Shrikian and A. K. Mapp, Org. Lett., 2010, 12, 2574; (d) O. Gutierrez, C. E. Hendrick and M. C. Kozlowski, Org. Lett., 2018, 20, 6539; (e) M. R. Siebert and D. J. Tantillo, J. Am. Chem. Soc., 2007, 129, 8686.
- 11 (a) J.-M. Begouin, J. E. M. N. Klein, D. Weickmann and B. Plietker, Top. Organomet. Chem., 2012, 38, 280; (b) Y.-N. Wang, L.-Q. Lu and W.-J. Xiao, Chem. - Asian J., 2018, 13, 2174; (c) Q. Cheng, H.-F. Tu, C. Zheng, J.-P. Qu, G. Helmchen and S.-L. You, Chem. Rev., 2019, **119**, 1855; (*d*) S. L. Rössler, D. A. Petrone and E. M. Carreira, *Acc.* Chem. Res., 2019, 52, 2657.
- 12 C. Hansch, A. Leo and R. W. Taft, Chem. Rev., 1991, 91, 165.
- 13 (a) J. W. Faller, M. E. Thomsen and M. J. Mattina, J. Am. Chem. Soc., 1971, 93, 2642; (b) G. Consiglio and R. M. Waymouth, Chem. Rev., 1989, 89, 257; (c) U. Kazmaier and F. L. Zumpe, Angew. Chem., Int. Ed., 2000, 39, 802.
- 14 S. Mizuno, H. Tsuji, Y. Uozumi and M. Kawatsura, Chem. Lett., 2020, 49, 645.
- 15 (a) Y. Zheng, C. M. Tice and S. B. Singh, Bioorg. Med. Chem. Lett., 2014, 24, 1673; (b) K. Hiesinger, D. Dar'in, E. Proschak and M. Krasavin, J. Med. Chem., 2021, 64, 150.
- 16 J. C. Jochims and F. A. Anet, J. Am. Chem. Soc., 1970, 92, 5524.
- 17 (a) C. Zheng, C.-X. Zhuo and S.-L. You, J. Am. Chem. Soc., 2014, 136, 16251; (b) J. A. Rossi-Ashton, A. K. Clarke, J. R. Donald, C. Zheng, R. J. K. Taylor, W. P. Unsworth and S.-L. You, Angew. Chem., Int. Ed., 2020, 59, 7598.
- 18 Calculated using IGMPlot. https://igmplot.univ-reims.fr. See: C. Levfebvre, H. Khartabil, J.-C. Boisson, J. Contreras-Garcia, J.-P. Piquemal and E. Hénon, Chem. Phys. Chem., 2018, 19, 724.